COMPUTING MULTIVALUED MATHEMATICAL MORPHOLOGY ON MULTI-BAND IMAGES USING ALGORITHMS FOR MULTICRITERIA ANALYSIS

L'HADDAD SAMIR[✉,1], KEMMOUCHE AKILA[1] AND TAÏBI AUDE NUSCIA[2]

[1]University of Sciences and Technology Houari Boumediene, Faculty of Electrical Engineering, Department of Telecommunication, BP32 El Alia Bab Ezzouar, Algiers, Algeria, 16111, [2]University of Angers, CNRS, ESO, SFR CONFLUENCES, 5 bis Boulevard Lavoisier, Angers, France, F-49000
e-mail: haddad.samir1985@gmail.com; akemmouche@usthb.com; audenousia.taibi@univ-angers.fr

ABSTRACT

Mathematical morphology (MM) is a powerful tool for spatial multispectral and hyperspectral image analyses. However, MM was originally developed for single-band images in which each pixel is represented by a numerical value. The most commonly used method for extending MM to multiband images is to process each band independently without considering its correlations with other bands. This can lead to the creation of artificial false spectral signatures and result in object misidentification. Therefore, extending MM to multiband images requires the use of an adequate vector ordering strategy to fully exploit its potential. This work proposes new vector ordering algorithms for the computation of multivalued MM. A multicriteria analysis (MCA) system is used as a tool for establishing an ordering of vectors. Two MCA approaches, namely, an "analytic hierarchy process" and a "preference ranking organization method for enrichment evaluation," are developed to define ordering relations between vectors. To ensure the validity of the proposed vector ordering algorithms, the computed multivalued morphological profiles are compared using the proposed vector ordering approaches and conventional schemes. The results of applying the proposed vector ordering algorithms for computing morphological profiles show that good classification accuracies were achieved for urban structures in ROSIS hyperspectral images.

Keywords: hyperspectral imaging, multiband images, multivalued mathematical morphology, multivalued morphological profile, vector ordering.

INTRODUCTION

Mathematical morphology (MM) is a useful tool for spatial image processing. The MM technique was developed by Serra (Serra, 1986; Nagel, 1988) and has been used to extract spatial information about the sizes, shapes, and orientations of objects present in single-band images. The two basic operations of mathematical morphology are erosion and dilation, which are formulated by the infimum operator (denoted as $\wedge$) and the supremum operator (denoted as $\vee$), respectively (Chevallier and Angulo, 2014). These two basic morphological operations are at the origins of more elaborate morphological transformations, such as morphological opening and closing by reconstruction (Soille, 2013). Initially, MM was defined for single-band images, where each pixel of the image is a scalar value and there is a natural ordering between the pixels in a predefined neighbourhood. However, it is less trivial to formulate pixel ordering relations in MM for multiband images. In fact, in multiband images, each pixel is a vector with m components corresponding to the pixel values of the m image bands, and scalar ordering is not possible. Therefore, the extension of MM to multiband images requires ordering among pixel vectors (Dougherty, 1992). Although several works have proposed extending MM to multiband images, there is no scientific consensus on the appropriate process. This is mainly because extending MM to multiband images is strongly related to the choice of an appropriate vector ordering scheme, which is considered an open mathematical problem (Aptoula and Lefèvre, 2007; Velasco-Forero and Angulo, 2011).

Barnett (1976) categorized the existing vector ordering algorithms used to extend MM to multiband images into four groups: marginal vector ordering strategies, conditional vector ordering strategies, reduced vector ordering strategies, and partial vector ordering strategies.

Marginal ordering strategies (M-ordering) process each image band of the original image separately from the other bands using scalar morphological operations and ignore the intercorrelations among image bands. Typically, due to the high dimensionality of images, marginal approaches are performed after the dimensionality reduction step to obtain a set of decorrelated bands (Li and Li, 2004; Benediktsson *et al.*, 2005). Examples of using marginal vector ordering strategies can be found in (Weber and Lefevre, 2008; Fauvel *et al.*, 2008; Chevallier *et al.*,

2016). Although marginal approaches are easy to use, they do not preserve vectors and can create new pixel vectors that are not present in the original image (Aptoula and Lefèvre, 2008b). This is mainly because a pixel vector is treated by marginal strategies as a collection of separate components rather than a single entity. In satellite images, this can lead to the creation of new spectral signatures and result in object misidentification.

Conditional ordering strategies (C-ordering) aim to rank vectors by assigning priorities to some (or all) vector components. This type of ordering is recommended for multiband images when the weights of some image bands are more important than others (Aptoula and Lefèvre, 2007). The efficiency of conditional algorithms depends on the chosen band prioritization function, which assigns weights (or priorities) to each image band in the conditional ordering scheme. Lexicographic ordering (L-ordering) is a specific C-ordering strategy inspired by the idea of sorting words in alphabetical order. In the lexicographic ordering scheme, vectors are initially ordered according to their first component values. Vectors with the same value at the first vector component are then ordered according to the next vector component values, and so on. It is also possible to obtain a valid lexicographic ordering scheme by inverting the priorities of the vector components (i.e., assigning higher weights to the last vector components and lower weights to the first vector components). L-ordering strategies guarantee that the supremum and infimum vectors are members of the initial set of compared vectors (i.e., the L-ordering preserves the original pixel vectors). These approaches also guarantee the uniqueness of the vector extremes (i.e., they find a unique supremum and a unique infimum for the compared vectors). However, lexicographic ordering strategies present the major drawback of exclusively using dominant vector components in their vector ordering decisions. Therefore, the remaining vector components rarely participate in the lexicographic ordering process (Aptoula and Lefèvre, 2008b). Despite this limitation, L-ordering imposes total order relations among the compared vectors (i.e., any two vectors can be compared and ordered) and has been widely used in several works, such as (Hanbury and Serra, 2001; Angulo, 2005; Aptoula and Lefevre, 2007; Aptoula and Lefèvre, 2008a; Angulo, 2010; Gao and Hu, 2013; Lei *et al.*, 2013).

Reduced ordering (R-ordering) strategies involve projecting multidimensional data onto a one-dimensional space and then applying the single-band MM approach. This projection is performed using an invertible rank function that produces a representative scalar value for each vector. The vectors are then ordered according to their associated scalar values. After applying single-band MM to the reduced data, the original multidimensional space is reconstructed by inverting the rank function that was initially used. R-ordering algorithms can utilize various predefined rank functions. These include simple rank functions such as PCA or other invertible dimensionality reduction algorithms (Chanussot and Lambert, 1998). Some approaches utilize different distance measures from predefined reference vectors as rank functions (Louverdis *et al.*, 2002; Al-Otum, 2003; Du *et al.*, 2003; Keshava, 2004; Van der Meer, 2006; Angulo, 2007; Garcia *et al.*, 2008). In certain R-ordering algorithms, the cumulative distance between each vector and all other vectors is computed to compare vectors, eliminating the need to choose a reference vector (Plaza *et al.*, 2002; 2004; 2005; 2009). Additionally, R-ordering strategies can be developed using other invertible rank functions, such as those presented in (Lezoray *et al.*, 2009; Lezoray and Elmoataz, 2012; Sangalli and Valle, 2019). Although the reduced ordering strategy takes the correlations between image bands into account and preserves the original vectors, the uniqueness of the vector extremes (i.e., finding only one infimum vector and/or only one supremum vector) is not guaranteed when the rank function is not injective (Louverdis *et al.*, 2002). To ensure the uniqueness of the vector extremes, an injective rank function should be used, or the reduced vector ordering process should be completed by an additional ordering relation to resolve the undecided cases (Angulo, 2007).

Partial vector ordering (P-ordering) strategies cluster a set of input vectors into groups of equivalence based on a predefined criterion. P-ordering strategies only compare vectors from two different (not identical) groups, which means that the resulting ordering relation is generally not a total relation. Furthermore, P-ordering approaches have the disadvantage of producing multiple vector extremes. Examples of using P-ordering strategies to extend MM to multiband images can be found in (Velasco-Forero and Angulo, 2011; 2012; Aptoula *et al.*, 2014; Velasco-Forero and Angulo, 2014; Franchi and Angulo, 2015).

A comprehensive overview of other works that have addressed the extension of mathematical morphology to multidimensional data is given in (Aptoula and Lefèvre, 2007; Van de Gronde and Roerdink, 2017).

According to the previously cited works, it follows that the definition of a multivalued MM requires an adequate vector ordering scheme. This scheme

should take the correlations between image bands into account and process all bands simultaneously. Vector preservation and the uniqueness of the vector extremes should be ensured. In addition, total order relations should be imposed between the compared vectors.

This paper addresses the problem of extending MM to multiband images by exploiting algorithms from the specific field of multicriteria analysis (MCA) systems. Two multicriteria analysis methods, the analytic hierarchy process (AHP) and the preference ranking organization method for enrichment evaluation (PROMETHEE), have been adapted to implement two new vector ordering algorithms for multivalued MM computing. For this purpose, the comparison structure of the exploited MCA approaches are utilized as vector comparison schemes to expand MM to multiband images. To our knowledge, no previous work has employed multicriteria analysis algorithms to design a vector ordering scheme, and even less to extend MM to multiband images. The resulting multivalued MM operators are used to construct morphological descriptors. The generated descriptors demonstrate better classification performance than that of conventional multivalued MM operators.

The remainder of this paper is organized as follows. The second section introduces multicriteria analysis systems and describes the two adapted multicriteria analysis algorithms. The third section discusses the experimental results. Finally, the conclusions of and new perspectives on this work are presented in Section 4.

MULTICRITERIA ANALYSIS SYSTEMS

Multicriteria analysis (MCA) systems are comparison systems that evaluate actions (alternatives, solutions or options) and select the optimal action that satisfies a maximum number of criteria for a predefined ranking objective (Roy *et al.*, 2002). The purpose of any multicriteria method is to reduce the incomparability (denoted as the R situation) between the compared actions as much as possible. A multicriteria analysis system is based on three key factors.

– Actions: An action is designated by an object on which the multicriteria decision is made. The set of potential actions in a multicriteria analysis system is denoted by A.

– Criteria: A criterion $g()$ is a function that assigns a utility value $g(a_i)$ for each action a_i. $g_k(a_i)$

designates the utility value (or the evaluation value) of action a_i according to the kth criterion. The elimination of superfluous and redundant criteria makes the multicriteria analysis process more robust (Roy *et al.*, 2002).

– Criteria weights: Some criteria may be more important than others. This importance is expressed by a weight coefficient in a multicriteria analysis system. A higher weight value designates a more privileged criterion. When the criteria have the same weights, the multicriteria system does not take the weights of the different criteria into account. In our work, w_k indicates the weight of the kth criterion.

To exploit a multicriteria analysis system for any type of problem, it is necessary to identify the previously mentioned factors (i.e., actions, criteria, and criteria weights), which are fundamental for utilizing the multicriteria analysis structure.

All multicriteria analysis methods start with the same evaluation matrix $D(n \times m)$, which is also called the judgement matrix or the performance matrix (see Eq. (1)), but they vary in their calculation procedures. Thus, the obtained results can differ from one multicriteria analysis method to another.

$$D_{(n \times m)} = \begin{pmatrix} g_1(a_1) & g_2(a_1) & \cdots & g_m(a_1) \\ g_1(a_2) & g_2(a_2) & \cdots & g_m(a_2) \\ \vdots & \vdots & \ddots & \vdots \\ g_1(a_n) & g_2(a_n) & \cdots & g_m(a_n) \end{pmatrix} \quad (1)$$

where the rows of the evaluation matrix D correspond to n compared actions and the columns correspond to m criteria. The element in the ith row and j^{th} column (i.e., $g_j(a_i)$) of the decision matrix D represents the utility value of the ith action a_i according to the jth criterion $g_j()$.

The purpose of this work is to consider the vector ordering problem as an MCA problem and to create a multicriteria representation of multiband data to exploit multicriteria analysis methods as vector ordering methods in multivalued MM computing settings.

To adapt a multicriteria comparison structure to the context of pixel vector ordering, we consider each pixel vector in a multiband image as an action a_i. Each image band is considered a criterion, and the spectral response of the pixel vector a_i for the kth image band is considered the utility value of action a_i according to the kth criterion in the MCA structure. The priority value of the kth image band represents the weight of the kth criterion (denoted as w_k). By specifying these

correspondences, the structure of the multiband image can be represented as a decision matrix in the MCA system. The pixel vectors are thus compared during the multivalued MM computation process by comparing their components in the MCA comparison structure.

The theoretical basis of MM imposes the use of a total ordering relation on the vector ranking process, even though this relation is more difficult to apply when the compared values do not have a one-dimensional structure (Dougherty, 1992; Serra, 1992). Therefore, using multicriteria analysis methods, which overcomes action incomparability (i.e., where two vectors with different components cannot be ordered), is more suitable in our work context.

Several multicriteria methods require additional information, such as predefined threshold values requiring human operator intervention (Greco *et al.*, 2016). In this paper, only automatic multicriteria analysis methods are employed.

According to the previous constraints, two multicriteria analysis methods, the AHP and PROMETHEE, are studied and developed to extend MM to multiband images. These methods are more commonly used for multicriteria analysis and are highly capable of extending MM to multiband images.

In the following subsections, we describe the two multicriteria analysis methods, the AHP and PROMETHEE, that are used for multivalued MM computing.

ANALYTIC HIERARCHY PROCESS (AHP)

The analytic hierarchy process (AHP) is a mathematical method for analysing and prioritizing a set of possible actions based on a predefined objective, from the best actions (i.e., those that satisfy the maximum number of criteria) to the worst actions. It was developed by Thomas L. Saaty (1987; 2008) and produces priority numbers for each action, quantifying its rank in the comparison set. It is important to note that the AHP output depends on the predefined objective, which can be oriented towards either maximization to find the supremum action or minimization to find the infimum action.

As previously mentioned, the AHP method starts with an evaluation matrix D (see Eq. (1)) that considers n actions and m evaluation criteria. For each criterion $g_k()$, the AHP creates a pairwise comparison matrix (called a binary comparison matrix) with a size of $(n \times n)$:

$$\begin{pmatrix} P^{(k)}_{(a_1,a_1)} & P^{(k)}_{(a_1,a_2)} & \cdots & P^{(k)}_{(a_1,a_n)} \\ P^{(k)}_{(a_2,a_1)} & P^{(k)}_{(a_2,a_2)} & \cdots & P^{(k)}_{(a_2,a_n)} \\ \vdots & \vdots & \ddots & \vdots \\ P^{(k)}_{(a_n,a_1)} & P^{(k)}_{(a_n,a_2)} & \cdots & P^{(k)}_{(a_n,a_n)} \end{pmatrix} \quad (2)$$

Each pairwise comparison matrix compares pairs of actions based on their scalar values according to the kth criterion. The element $P^{(k)}_{(a_i,a_j)}$ in the matrix represents the preference, or dominance, of action a_i over action a_j with respect to the kth criterion. If two actions have the same preference in the pairwise comparison matrix, the entry $P^{(k)}_{(a_i,a_j)}$ is equal to 1. The preference $P^{(k)}_{(a_i,a_i)}$ is always 1 for all $i = 1, \cdots, n$. Note that the entries $P^{(k)}_{(a_i,a_j)}$ and $P^{(k)}_{(a_j,a_i)}$ satisfy the following formula:

$$P^{(k)}_{(a_i,a_j)} = \frac{1}{P^{(k)}_{(a_j,a_i)}} \quad (3)$$

In the AHP technique, the relative preference $P^{(k)}_{(a_i,a_j)}$ between two actions a_i and a_j according to criterion $g_k()$ is quantified according to the numerical Saaty scale, which ranges from 1 to 9. Level 1 corresponds to equal preference for both actions, while level 9 corresponds to the absolute preference of one action over another. The intermediate values between these two limits represent intermediate preference values. However, for our vector ordering approach, the Saaty scale is not appropriate because it is too restrictive, relies on a human factor when attributing preference values, and ignores the distance measurements between two vectors. Therefore, we replace the classic AHP scale with a new preference function $P^{(k)}$ (see Eq. (4)) that uses a distance measurement without considering any reference vector.

$$\begin{cases} \text{if } g_k(a_i) > g_k(a_j) & \text{then } P^{(k)}_{(a_i,a_j)} = (g_k(a_i) - g_k(a_j)) + 1 \\ \text{if } g_k(a_i) < g_k(a_j) & \text{then } P^{(k)}_{(a_i,a_j)} = \frac{1}{(g_k(a_j) - g_k(a_i))} \\ \text{if } g_k(a_i) = g_k(a_j) & \text{then } P^{(k)}_{(a_i,a_j)} = 1 \end{cases}$$

$$(4)$$

The preference function $P^{(k)}$ proposed in Eq. (4) is utilized only when searching for the supremum pixel vector (i.e., maximizing the ranking objective). On the other hand, when searching for the infimum pixel vector (i.e., minimizing the ranking objective),

the preference function must be inverted as shown in Eq. (5).

$$
\begin{cases}
\text{if } g_k(a_i) < g_k(a_j) & \text{then } P^{(k)}_{(a_i,a_j)} = (g_k(a_j) - g_k(a_i)) + 1 \\
\text{if } g_k(a_i) > g_k(a_j) & \text{then } P^{(k)}_{(a_i,a_j)} = \dfrac{1}{(g_k(a_i) - g_k(a_j))} \\
\text{if } g_k(a_i) = g_k(a_j) & \text{then } P^{(k)}_{(a_i,a_j)} = 1
\end{cases}
\tag{5}
$$

After constructing the pairwise comparison matrix for the kth criterion, it is normalized using the following formula:

$$
\overline{P}^{(k)}_{(a_i,a_j)} = \frac{P^{(k)}_{(a_i,a_j)}}{\sum_{l=1}^{n} P^{(k)}_{(a_l,a_j)}}
\tag{6}
$$

This normalization process results in preference values that lie within the interval of $[0,1]$.

To determine the priority of each action a_i based on the kth criterion (denoted as $\alpha_i^{(k)}$) while considering the normalized pairwise comparison matrix, the following formula can be used:

$$
\alpha_i^{(k)} = \frac{\sum_{l=1}^{n} \overline{P}^{(k)}_{(a_i,a_l)}}{n}
\tag{7}
$$

To quantify the overall priority of each action a_i for all criteria simultaneously, the numerical overall priority of each action is calculated using the following formula:

$$
P_{(a_i)} = (\alpha_i^{(1)} \times w_1) + \cdots + (\alpha_i^{(k)} \times w_k) + \cdots + (\alpha_i^{(m)} \times w_m)
\tag{8}
$$

The computed overall priority $P_{(a_i)}$ indicates the relative importance of an action a_i compared to all other actions according to the predefined ranking objective. The overall action priorities (Eq. (8)) lead to an AHP ranking list of the compared actions. This list facilitates the selection of the most dominant action (i.e., the action that maximizes the overall priority) according to the predefined ranking objective. The AHP method treats the multicriteria problem using the same steps for both ranking objectives (i.e., for the maximization and minimization objectives), only adapting the preference function in the binary pairwise comparison matrix to the chosen ranking objective.

In the AHP preference architecture, it is possible to rank actions without using the relative criteria coefficients. In this particular case, all criteria have the same weight ($w_k = 1/m \ \forall \ k \in [1,m]$) in the multicriteria analysis system. Both scenarios, using different or similar criteria weights, are considered in this paper.

The AHP is a complete aggregation method that converts various action evaluations obtained according to the set of criteria into a unique numerical number that reflects the overall prioritization of this action. Thus, the proposed ordering algorithm using the AHP method can be considered a reduced vector ordering approach since pixel vectors are compared by the AHP based on their aggregated numerical values (i.e., their overall priority indices).

PREFERENCE RANKING ORGANIZATION METHOD FOR ENRICHMENT EVALUATION (PROMETHEE)

Jean-Pierre Brans and Philippe Vincke developed the PROMETHEE ranking method (Brans, 1985; Brans *et al.*, 1986) to address multicriteria problems where conflicting criteria must be considered. This method enables a finite number of actions to be ranked based on several criteria.

The first step of the PROMETHEE method is to construct an evaluation matrix $D(n \times m)$ (see Eq. (1)), which allows actions to be compared.

The preference structure of the PROMETHEE method is constructed from the evaluation matrix $D(n \times m)$ by making pairwise action comparisons. To compare two actions a_i and a_j via PROMETHEE according to a criterion $g_k()$, their preference degree (or preference intensity) $PF^{(k)}_{(a_i,a_j)}$, which can vary between 0 and 1, is evaluated. The preference function $PF^{(k)}$ used to estimate the preference degree between two actions takes the distance d_k between the compared actions a_i and a_j into account, as shown in the following equations:

$$
PF^{(k)}_{(a_i,a_j)} = PF^{(k)}(d_k(a_i,a_j))
\tag{9}
$$

where

$$
d_k(a_i,a_j) = g_k(a_i) - g_k(a_j)
\tag{10}
$$

The preference degree $PF^{(k)}_{(a_i,a_j)}$ between two actions a_i and a_j determined according to criterion $g_k()$ is influenced by the distance d_k between them. A small distance results in a small preference, while a large distance leads to a large preference. When the distance d_k is null or negligible, there is no preference for either of the two compared actions.

Table 1: *The Six Brans and Vincke Preference Functions.*

Preference functions	Mathematical Expression for the Maximization Ranking Objective	Thresholds Used by the Preference Function
Usual function	$PF_{(a_i,a_j)}^{(k)} = \begin{cases} 0 & \text{if } d_k(a_i,a_j) \leq 0 \\ 1 & \text{if } d_k(a_i,a_j) > 0 \end{cases}$	No threshold
U-shaped function	$PF_{(a_i,a_j)}^{(k)} = \begin{cases} 0 & \text{if } d_k(a_i,a_j) \leq q_k \\ 1 & \text{if } d_k(a_i,a_j) > q_k \end{cases}$	Indifference threshold q_k
V-shaped function	$PF_{(a_i,a_j)}^{(k)} = \begin{cases} 0 & \text{if } d_k(a_i,a_j) \leq 0 \\ \dfrac{d_k(a_i,a_j)}{p_k} & \text{if } 0 < d_k(a_i,a_j) \leq p_k \\ 1 & \text{if } d_k(a_i,a_j) > p_k \end{cases}$	Preference threshold p_k
Level function	$PF_{(a_i,a_j)}^{(k)} = \begin{cases} 0 & \text{if } d_k(a_i,a_j) \leq q_k \\ \dfrac{1}{2} & \text{if } q_k < d_k(a_i,a_j) \leq p_k \\ 1 & \text{if } d_k(a_i,a_j) > p_k \end{cases}$	Indifference threshold q_k + Preference threshold p_k
Linear function	$PF_{(a_i,a_j)}^{(k)} = \begin{cases} 0 & \text{if } d_k(a_i,a_j) \leq q_k \\ \dfrac{d_k(a_i,a_j) - q_k}{p_k - q_k} & \text{if } q_k < d_k(a_i,a_j) \leq p_k \\ 1 & \text{if } d_k(a_i,a_j) > p_k \end{cases}$	Indifference threshold q_k + Preference threshold p_k
Gaussian function	$PF_{(a_i,a_j)}^{(k)} = \begin{cases} 0 & \text{if } d_k(a_i,a_j) \leq 0 \\ 1 - (\exp{-(\frac{d_k(a_i,a_j)^2}{2\sigma_k^2})}) & \text{if } d_k(a_i,a_j) > 0 \end{cases}$	Gaussian threshold σ_k (an intermediate value between q_k and p_k)

Choosing an appropriate preference function $PF^{(k)}$ is a crucial step since the results of the PROMETHEE method depend on this function. Table 1 summarizes the six preference functions proposed by Brans (1985) for the PROMETHEE multicriteria method: the usual function, U-shaped function, V-shaped function, level function, linear function, and gaussian function.

The preference functions reported in Table 1 are defined for the maximization objective. In the case of minimization (i.e., when searching for the infimum pixel vector), it is sufficient to reverse the selected preference function.

After selecting a preference function $PF^{(k)}$, an aggregated preference index $\sqcap P\,(a_i,a_j)$ is computed for each pair of compared actions (a_i,a_j) (see Eq. (11)).

The index $\sqcap P\,(a_i,a_j)$ gives the degree to which an alternative a_i is preferred over another alternative a_j when simultaneously considering all criteria:

$$\sqcap P\,(a_i,a_j) = \sum_{k=1}^{m} (PF_{(a_i,a_j)}^{(k)} \times w_k) \qquad (11)$$

An aggregated preference index $\sqcap P\,(a_i,a_j)$ close to 0 (close to 1) implies a weak preference (strong preference) for action a_i over action a_j when simultaneously considering all the criteria. Therefore, with n actions, there are $(n-1)$ aggregated preference indices for each action a_i.

The criterion weight w_k is considered when computing the $\sqcap P$ index. In the PROMETHEE method, the criteria can have the same weights (*i.e.*, $w_k = 1/m \; \forall \; k \in [1,m]$) or different weights in Eq. (11). It should be noted that both scenarios are considered in our experimental section.

The next step in the PROMETHEE method is to determine the outranking relations between the compared actions. This involves computing three outranking flows for each action a_i.

The first is the positive outranking flow Φ^+. The Φ^+ flow reflects how action a_i outranks and dominates all the other actions according to the predefined ranking objective. It corresponds to the outranking characteristic of action a_i and is defined as follows:

$$\Phi_{a_i}^+ = \frac{1}{n-1} \sum_{x \in A} \sqcap P(a_i,x) \qquad (12)$$

where n is the number of actions in the comparison set A.

The second outranking flow is the negative outranking flow Φ^-. The Φ^- flow reflects how action a_i is outranked and dominated by all other actions according to the predefined ranking objective. It corresponds to the outranked characteristic of action a_i and is computed by:

$$\Phi_{a_i}^- = \frac{1}{n-1} \sum_{x \in A} \sqcap P(x, a_i) \tag{13}$$

The net flow Φ (also called the global flow) is defined as the arithmetic difference between the positive and negative flows:

$$\Phi_{a_i} = \Phi_{a_i}^+ - \Phi_{a_i}^- \tag{14}$$

The net flow is a measure of the overall outranking degree of an action a_i compared to the other actions in the comparison set A.

To designate final action rankings, PROMETHEE considers the net flow Φ values associated with the compared actions. For all compared actions, there are two possible ranking relations:

$$\begin{cases} [a_i \, P \, a_j] & \text{if } \Phi_{a_i} > \Phi_{a_j} \\ [a_i \, I \, a_j] & \text{if } \Phi_{a_i} = \Phi_{a_j} \end{cases} \tag{15}$$

Here, P and I are the preference and indifference situations, respectively, between the two actions a_i and a_j. Note that there is no incomparability situation involving the compared actions. This approach provides a complete ranking relation in the comparison architecture and is highly capable of extending MM to multivalued images (Talbot *et al.*, 1998).

The best preferred action according to the ranking objective (the maximization or minimization objective) is the action with the greatest net flow, which is selected by the PROMETHEE method.

As previously mentioned, the PROMETHEE method uses a preference function $PF^{(k)}$ to conduct binary comparisons (see Table 1). The following part of this subsection describes the preference functions used by PROMETHEE in the present work.

In this paper, the first utilized preference function is the standard usual function (see Table 1). It is a binary function that does not use any threshold and takes only two values: 0 for the indifference situation between two actions and 1 for the total (or strict) preference situation in favour of one action. The usual function defined in Table 1 must be reversed for the minimization context so that the formula for $PF^{(k)}_{(a_i, a_j)}$ becomes:

$$PF^{(k)}_{(a_i, a_j)} = \begin{cases} 0 & \text{if } d_k(a_i, a_j) \geq 0 \\ 1 & \text{if } d_k(a_i, a_j) < 0 \end{cases} \tag{16}$$

The usual preference model suggests that even the smallest differences $d_k(a_i, a_j)$ between actions can indicate a preference situation.

To address this, we also use the U-shaped function (see Table 1) in the PROMETHEE preference architecture. The U-shaped function considers a small distance $d_k(a_i, a_j)$ between actions as an indication of indifference between the two actions for a given criterion $g_k()$. The indifference interval is delimited by the indifference threshold value q_k, above which there is indifference and below which there is a total (or strict) preference situation.

Employing the U-shaped preference model requires the value of the indifference threshold q_k to be determined, which is not a trivial task and is usually performed by a human operator. However, we develop a strategy to use the U-shaped preference function without specifying any indifference threshold value for the q_k parameter. This strategy is summarized by the following formula:

$$PF^{(k)}_{(a_i, a_j)} = \begin{cases} 0 & \text{if } d_k(a_i, a_j) < 0 \\ & \text{or } d_k(a_i, a_j) \geq 0 \text{ and } d_k(a_i, a_j) \leq 0.1 \cdot g_k(a_i) \\ 1 & \text{if } d_k(a_i, a_j) \geq 0 \text{ and } d_k(a_i, a_j) > 0.1 \cdot g_k(a_i) \end{cases} \tag{17}$$

where $0.1 \cdot g_k(a_i)$ corresponds to 10% of $g_k(a_i)$.

When the ranking objective is to search for the infimum extreme, the curve of the U-shaped preference function must be inverted as follows:

$$PF^{(k)}_{(a_i, a_j)} = \begin{cases} 0 & \text{if } d_k(a_i, a_j) \geq 0, \\ & \text{or } d_k(a_i, a_j) < 0 \text{ and } |d_k(a_i, a_j)| \leq 0.1 \cdot g_k(a_j) \\ 1 & \text{if } d_k(a_i, a_j) < 0 \text{ and } |d_k(a_i, a_j)| > 0.1 \cdot g_k(a_j) \end{cases} \tag{18}$$

The U-shaped function expresses indifference between two actions or a strict preference (i.e., a total preference or strong preference) for one action. Therefore, the U-shaped preference model is unable to distinguish between strong and weak preference situations.

In contrast, the V-shaped, level, and linear preference functions (see Table 1) consider both strong and weak preference situations in the preference model by using two distinct thresholds: an indifference threshold q_k, below which there is indifference between two compared actions, and a preference threshold p_k, above which there is a strong preference

for one of the two compared actions. These two thresholds define an intermediate zone that represents weak preference and marks the transition between the indifference and strong preference situations. However, it can be challenging to determine the optimal values for q_k and p_k.

To avoid predefining the q_k and p_k thresholds, we apply our elaborated strategy from the previous U-shaped function to the level preference function. We discard the use of the V-shaped and linear preference functions in this work because they require predefined values for q_k and p_k in the preference value computation (see Table 1), which is not the case for the level preference function. Therefore, our proposed preference architecture using the level preference function is defined as follows:

$$PF_{(a_i,a_j)}^{(k)} = \begin{cases} 0 & \text{if } d_k(a_i,a_j) < 0 \\ & \text{or } d_k(a_i,a_j) \geq 0 \text{ and } d_k(a_i,a_j) \leq 0.1 \cdot g_k(a_i) \\ \frac{1}{2} & \text{if } d_k(a_i,a_j) \geq 0 \text{ and } 0.1 \cdot g_k(a_i) < d_k(a_i,a_j) \\ & \text{and } d_k(a_i,a_j) \leq 0.4 \cdot g_k(a_i) \\ 1 & \text{if } d_k(a_i,a_j) \geq 0 \text{ and } d_k(a_i,a_j) > 0.4 \cdot g_k(a_i) \end{cases}$$
(19)

where $0.1 \cdot g_k(a_i)$ and $0.4 \cdot g_k(a_i)$ correspond to 10% and 40% of $g_k(a_i)$, respectively.

When the ranking objective is to search for the infimum extreme, the curve of the level preference function must be inverted in the same way as that applied to the U-shaped preference function.

The percentage values (0.1 for 10% and 0.4 for 40%) used in the level (see Eq. (19)) and U-shaped (see Eq. (17) and Eq. (18)) preference functions are experimentally determined and found to be effective for the tested data. Different percentage values can be used to delimit the indifference, strict preference, and weak preference intervals. However, this topic is not the focus of this paper.

The Gaussian preference function is another preference function that takes both strong and weak preference situations into account without requiring the specification of indifference thresholds (q_k) or preference thresholds (p_k) (see Table 1). The Gaussian preference function allows preferences to vary progressively from totally weak (nonexistent preferences, i.e., $PF_{(a_i,a_j)}^{(k)} = 0$) to totally strong (strict preferences, i.e., $PF_{(a_i,a_j)}^{(k)} = 1$), passing through the intermediate preference values between these two extremes. The Gaussian preference function is associated with a Gaussian threshold σ_k, which is defined as:

$$\sigma_k = \sqrt{\frac{(g_k(a_i) - \frac{d_k(a_i,a_j)}{2})^2 + (g_k(a_j) - \frac{d_k(a_i,a_j)}{2})^2}{2}} \quad (20)$$

When searching for the infimum extreme (i.e., searching for the infimum pixel vector), the Gaussian preference function must be inverted as follows:

$$PF_{(a_i,a_j)}^{(k)} = \begin{cases} 0 & \text{if } d_k(a_i,a_j) \geq 0 \\ 1 - (\exp{-(\frac{d_k(a_i,a_j)^2}{2\sigma_k^2})}) & \text{if } d_k(a_i,a_j) < 0 \end{cases}$$
(21)

The PROMETHEE method is an aggregation technique that combines diverse action evaluations determined by criteria into a single numerical value that represents the overall action prioritization. As a result, the proposed ordering algorithm utilizing the PROMETHEE method can be viewed as a reduced vector ordering approach since pixel vectors are compared by the PROMETHEE method based on their aggregated numerical values (i.e., their net flows).

In the previous section, we adapted two MCA methods to our goal of ordering vectors in multivalued MM computing process.

In the next section, we use the vector ordering algorithms proposed based on the two presented multicriteria analysis methods to generate spatial descriptors using a multivalued morphological profile (multivalued MP). A comparison between the classification results obtained from the proposed methods and those obtained from conventional vector ordering methods is discussed in the following section.

EXPERIMENTAL RESULTS

This section aims to evaluate the efficiency of the proposed vector ordering algorithms by comparing the classification rates achieved using spatial morphological descriptors. The morphological descriptors are obtained by performing multivalued MP computations using the proposed and conventional vector ordering methods.

The multivalued MP (Benediktsson *et al.*, 2003; 2005) generates morphological descriptors through successive morphological opening and closing by reconstruction with a structuring element (SE) possessing an increasing size.

For the multivalued MP computations, we consider seven vector ordering algorithms:

– The lexicographic vector ordering algorithm with decreasing band weights

– The lexicographic vector ordering algorithm with increasing band weights

– The proposed AHP-based vector ordering algorithm

– The proposed PROMETHEE vector ordering algorithm using the usual preference function

– The proposed PROMETHEE vector ordering algorithm using the U-shaped preference function

– The proposed PROMETHEE vector ordering algorithm using the level preference function

– The proposed PROMETHEE vector ordering algorithm using the Gaussian preference function

In all the experiments, widely known conventional vector ordering schemes, namely, lexicographic vector ordering schemes with decreasing and increasing band weights, are used as comparison methods to validate the proposed vector ordering algorithms. These conventional schemes are chosen as comparison references due to their efficiency, simplicity, and common use in multivalued morphological image analysis cases. These methods do not require parameters and intuitively ordered image bands. Additionally, the total order relation in the vector comparison method is well suited for multivalued MMs (Talbot *et al.*, 1998) and is guaranteed by the lexicographic vector ordering algorithms, as noted in previous studies (Hanbury and Serra, 2001; Angulo, 2007; 2010).

The experimental results are obtained using two multiband images acquired by ROSIS sensors over the Pavia region in northern Italy. The images cover a complex urban environment with a spatial resolution of 1.3 metres and consist of 103 spectral bands for Pavia University and 102 spectral bands for Pavia Center (after the water absorption and noisy bands are removed) (Tarabalka *et al.*, 2009; 2010).

The multiband image of Pavia University consists of 610*340 pixels and has a ground-truth image that distinguishes the nine land cover classes on the university campus: asphalt, meadows, gravel, trees, painted metal sheets, bare soil, bitumen, bricks, and shadows. Fig. 1 (a) and Fig. 1 (b) show the true colour composites of the original multiband image and the available ground-truth regions, respectively.

The multiband image of the Pavia Center has spatial dimensions of 1096 by 715 pixels and has a ground-truth map that distinguishes eight different classes of urban objects: asphalt, meadows, trees, bare soil, bitumen, brick roofs, parking lots, and water. Figure 2 displays the Pavia Center image and its corresponding ground-truth image.

The number of pixels per class composing the ground-truth images is reported in Table 2 for the Pavia University scene and in Table 3 for the Pavia Center scene.
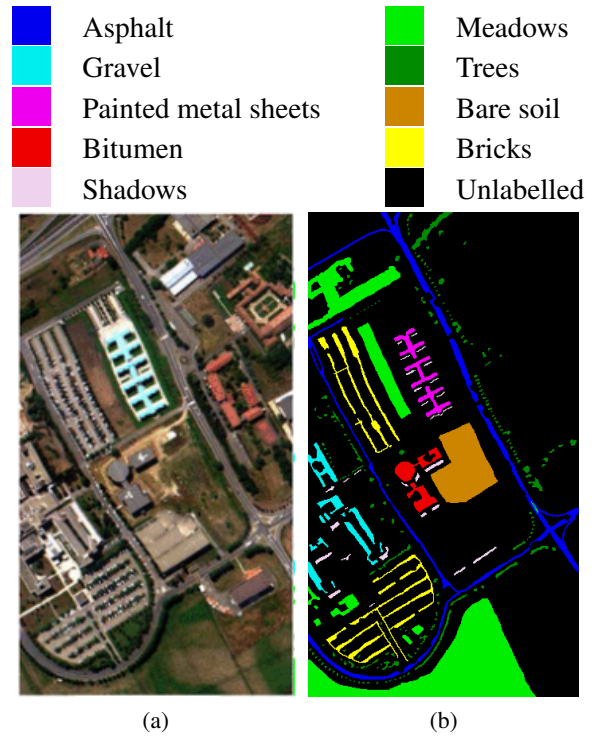

Fig. 1: *Pavia University Scene. (a) True colour composite of the original image. (b) Ground-truth image with nine land cover classes: asphalt, meadows, gravel, trees, painted metal sheets, bare soil, bitumen, bricks, and shadows.*

Before implementing the multivalued MP computation, dimensionality reduction is applied to the original multiband images using principal component analysis (PCA). This step eliminates redundant and highly correlated bands that represent superfluous criteria and may compromise the robustness of the multicriteria analysis process (Roy *et al.*, 2002).

Thus, only the first three PCA components from each image, which capture the majority of the spatial information and account for more than 99% of the total eigenvalues (as indicated in Tables 4 and 5), are utilized for computing the multivalued MP.

Note that the percentages of the eigenvalues of the selected PCA components in each reduced image are considered the band weights (i.e., criteria weights) in the multicriteria analysis architecture.
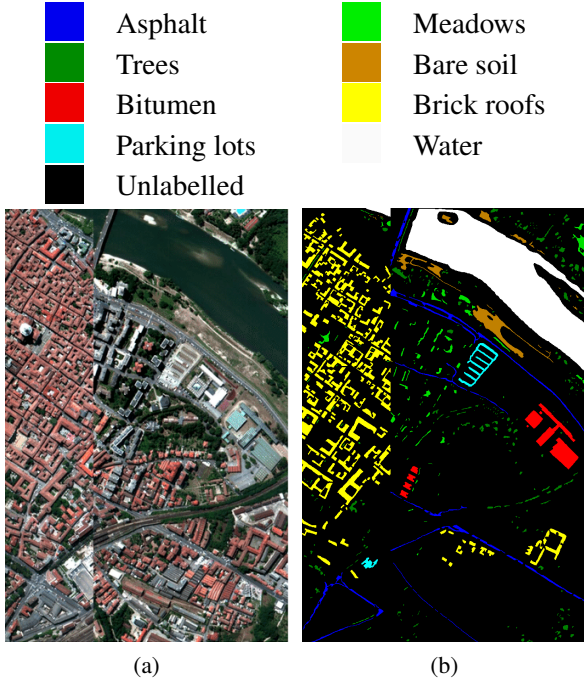
(a)   (b)

Fig. 2: *Pavia Center Scene. (a) The true colour composite of the original image. (b) The ground-truth image with eight land cover classes: asphalt, meadows, trees, bare soil, bitumen, brick roofs, parking lots, and water.*

Table 2: *Ground-truth classes and numbers of test samples for the Pavia University Scene.*

Class	Number of test samples
Asphalt	6631
Meadows	18649
Gravel	2099
Trees	3064
Painted metal sheets	1345
Bare soil	5029
Bitumen	1330
Bricks	3682
Shadows	947

The effectiveness of the compared vector ordering algorithms is evaluated using the support vector machine (SVM) classifier (Vapnik, 1998). The SVM classification results are quantified using three metrics, namely, the overall accuracy (OA), the individual test accuracy (ITA), and the kappa statistic rate (Rosenfield and Fitzpatrick-Lins, 1986; Congalton, 1991; Congalton and Green, 2019). High OA, ITA, and the kappa coefficient values indicate accurate classification results (Congalton, 1991).

Table 3: *Ground-truth classes and numbers of test samples for the Pavia Center Scene.*

Class	Number of test samples
Asphalt	9248
Meadows	3090
Trees	7598
Bare soil	6584
Bitumen	7287
Brick Roofs	42826
Parking Lot	2685
Water	65971

Table 4: *Eigenvalues and percentages of cumulative spatial information for the PCA components of the Pavia University Scene.*

The PCA components	Eigenvalues of the PCA components	Percentage of cumulative variance $(\lambda_k / \sum_{l=1}^{103} \lambda_l)$
λ_1	3.13×10^7	58.32%
λ_2	1.94×10^7	36.10%
λ_3	0.25×10^7	4.72%
$\lambda_4 + \lambda_5 + \cdots + \lambda_{103}$	0.046×10^7	0.86%

Table 5: *Eigenvalues and percentages of cumulative spatial information for the PCA components of the Pavia Center Scene.*

The PCA components	Eigenvalues of the PCA components	Percentage of cumulative variance $(\lambda_k / \sum_{l=1}^{102} \lambda_l)$
λ_1	4.51×10^7	70.23%
λ_2	1.67×10^7	26.07%
λ_3	0.18×10^7	2.83%
$\lambda_4 + \lambda_5 + \cdots + \lambda_{102}$	0.056×10^7	0.87%

Spectral SVM classification is normally conducted using the spectral bands of the reduced images. Instead, spatial-spectral SVM classification uses both spectral information and the spatial information computed from multivalued MMs via seven compared vector ordering algorithms.

The next subsections will discuss the classification results obtained for both the Pavia University and Pavia Center scenes.

Table 6: *Classification accuracies (percentages) achieved by different vector ordering algorithms using various criteria weights for the Pavia University image.*

Land Cover Classes	Reduced image (spectral classification)	Lexicographic ordering with decreasing band weights	Lexicographic ordering with increasing band weights	AHP with various criteria weights	PROMETHEE using the usual preference function with various criteria weights	PROMETHEE using the U-shaped preference function with various criteria weights	PROMETHEE using the level preference function with various criteria weights	PROMETHEE using the Gaussian preference function with various criteria weights
Asphalt	97.20	97.95	98.31	97.62	97.39	97.99	97.84	98.16
Meadows	93.55	95.77	97.75	98.54	96.92	96.11	95.78	97.16
Gravel	43.32	72.32	54.30	83.15	75.27	79.58	85.88	85.58
Trees	82.85	79.59	67.59	85.67	91.35	89.64	87.99	85.42
Painted metal	96.48	97.74	86.93	98.53	97.55	95.79	97.71	98.37
Bare soil	77.37	84.52	84.02	88.07	85.99	87.99	87.25	87.48
Bitumen	56.65	81.72	55.20	88.44	75.51	81.52	85.27	82.30
Bricks	84.41	90.83	86.80	89.76	86.99	87.20	86.15	88.50
Shadows	73.17	78.80	70.78	85.88	77.51	80.06	83.86	86.18
OA	82.82	90.53	85.36	93.34	90.81	91.47	92.06	92.69
Kappa	0.76	0.87	0.81	0.91	0.88	0.89	0.90	0.90

Table 7: *Classification accuracies (percentage) attained by different vector ordering algorithms using the same criteria weights for the Pavia University image.*

Land Cover Classes	Reduced image (spectral classification)	Lexicographic ordering with decreasing band weights	Lexicographic ordering with increasing band weights	AHP with the same criteria weights	PROMETHEE using the usual preference function with the same criteria weights	PROMETHEE using the U-shaped preference function with the same criteria weights	PROMETHEE using the level preference function with the same criteria weights	PROMETHEE using the Gaussian preference function with the same criteria weights
Asphalt	97.20	97.95	98.31	97.24	97.74	97.60	96.97	97.18
Meadows	93.55	95.77	97.75	95.56	94.57	94.54	95.90	94.23
Gravel	43.32	72.32	54.30	67.11	43.42	45.72	51.07	64.14
Trees	82.85	79.59	67.59	84.84	84.59	85.15	81.28	84.76
Painted metal	96.48	97.74	86.93	97.16	97.11	94.53	97.55	96.88
Bare soil	77.37	84.52	84.02	83.32	79.92	79.96	80.72	82.53
Bitumen	56.65	81.72	55.20	58.96	50.92	52.21	57.86	61.84
Bricks	84.41	90.83	86.80	87.30	85.85	87.48	85.52	86.91
Shadows	73.17	78.80	70.78	79.87	77.11	78.39	79.83	83.65
OA	82.82	90.53	85.36	87.31	83.83	84.35	85.51	86.93
Kappa	0.76	0.87	0.81	0.83	0.79	0.79	0.81	0.83

Experiment 1: Pavia University scene

Table 6 and Table 7 provide a summary of the results obtained by the proposed vector ordering algorithms in two different scenarios: one where the criteria weights vary and another where they are similar. The first column of each table reports the spectral classification accuracies attained for the Pavia University scene using the SVM classifier.

The results show that using only spectral information yields an OA of 82.82% and a kappa coefficient of 0.76. However, incorporating the spatial information obtained through the multivalued MP

significantly improves the classification accuracies in terms of both the OA and kappa rates, regardless of the vector ordering scheme used in the multivalued MP computation.

Table 6 shows that using various criteria weights in the proposed multicriteria vector ordering algorithms results in significantly higher classification accuracies than those of the conventional algorithms, with an OA rate of up to 90.80% and a kappa rate of 0.87. In contrast, when using the same criteria weights, the proposed multicriteria vector ordering algorithms result in lower classification rates than does conventional lexicographic vector ordering with decreasing band weights, as shown in Table 7.

The results also show that the classification results of the PROMETHEE vector ordering algorithm vary depending on the preference function used in the PROMETHEE preference architecture, as illustrated in the last four columns of Table 6 and Table 7.

The Gaussian preference function yields the highest overall accuracy, followed by the level preference function, which is comparable to the Gaussian function, particularly when considering various criteria weights. However, the usual preference function yields lower OA and kappa values for the PROMETHEE method, possibly because the conventional Boolean logic of the usual preference model excludes the intermediate level between strong and weak preferences when comparing pixel vectors.

On the Pavia University dataset, the AHP-based vector ordering method yields the best OA and kappa classification rates, regardless of whether the same or various criteria weights are used in the multicriteria vector ordering architecture.

Considering the individual test accuracy (ITA) rates, the influence of each vector ordering algorithm on the individual classification results varies for different thematic classes.

By comparing Tables 6 and 7, it is found that when using various criteria weights in the multicriteria vector ordering scheme, the proposed vector ordering algorithms result in higher accuracies for most classes. This is especially true for the gravel and asphalt land cover types, which exhibit greater sensitivity to class-specific accuracies for the criteria weighting parameter.

When the proposed methods using the same criteria weights are compared to the two conventional lexicographic vector ordering methods, it is found that the lexicographic methods outperform the proposed methods for the majority of the land cover classes. However, the use of various criteria weights in the

multicriteria vector ordering algorithms significantly outperforms the lexicographic methods for 8 land cover classes, including meadows, trees, bare soil, brick roofs, parking lots, and water.

Among the proposed multicriteria vector ordering algorithms that use various criteria weights, the PROMETHEE method combined with a Gaussian preference function and the AHP algorithm increase the discrimination potential for individual classes. However, several exceptions are noted, such as the asphalt land cover type, which yields better individual test accuracy for the conventional lexicographic vector ordering algorithm with decreasing band weights (98.31%); the brick class, which registers higher individual test accuracy for the lexicographic vector ordering algorithm with increasing band weights (90.83%); and the high individual classification accuracy obtained by the PROMETHEE vector ordering algorithm with the U-shaped preference function (91.35%) for the tree class.

The individual test accuracies obtained for different land cover classes with the proposed vector ordering algorithms using various criteria weights and the same criteria weights are presented in Fig. 3 and Fig. 4, respectively.

Experiment 2: The Pavia Center scene

The Pavia Center scene is an image of an urban area that contains small and closely spaced structures. Tables 8 and 9 summarize the overall accuracies (OA), individual classification accuracies (ITA), and Kappa coefficients achieved for the Pavia Center image and show that the classification process using the spatial information obtained by different vector ordering algorithms provides some classification improvement over the spectral strategy. This classification improvement may or may not be significant, depending on the vector ordering algorithm used in the multivalued MP computing task.

Comparing Tables 8 and 9, we can see the that multicriteria vector ordering algorithms incorporating various criteria weights are not only more efficient than those using the same criteria weights but also more efficient than the conventional lexicographic vector ordering methods.

The PROMETHEE method using the Gaussian function outperforms all other vector ordering approaches in both cases (using the same or various criteria weights).

The impact of each vector ordering algorithm on the individual classification results varies for different thematic classes, as indicated by the individual test accuracy (ITA) rates.
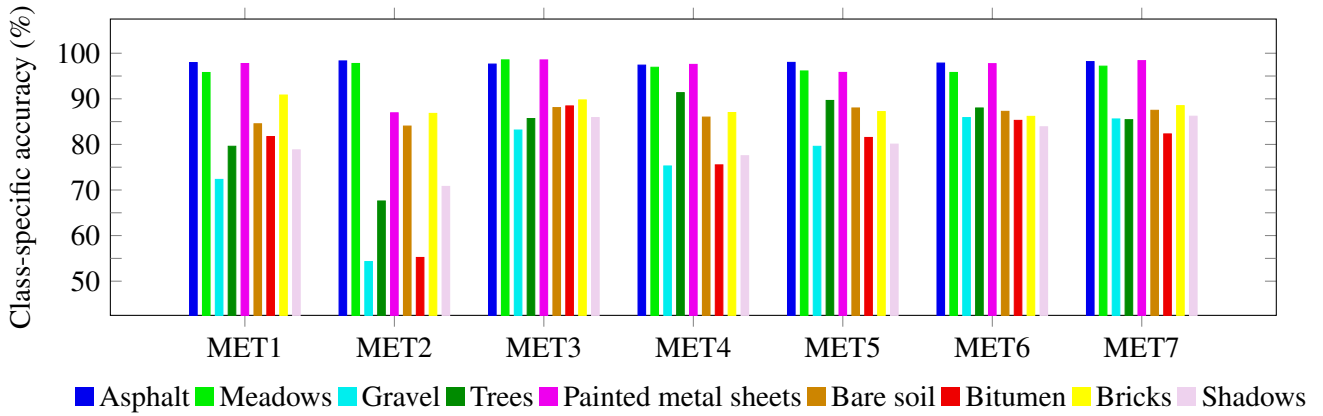
Fig. 3: *Individual test accuracies achieved for nine land-cover classes using the proposed vector ordering algorithms with various criteria weights (MET1: lexicographic ordering with decreasing weights, MET2: lexicographic ordering with increasing weights, MET3: the AHP method, MET4: PROMETHEE method with the usual preference function, MET5: the PROMETHEE method with the U-shaped preference function, MET6: the PROMETHEE method with the level preference function, and MET7: the PROMETHEE method with the Gaussian preference function).*
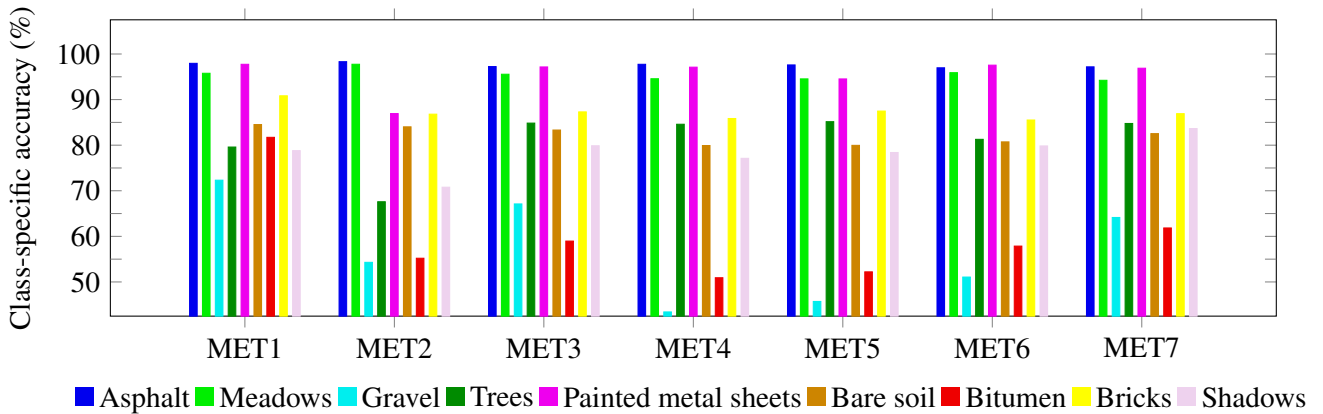

Fig. 4: *Individual test accuracies achieved for nine land cover classes using the proposed vector ordering algorithms with the same criteria weights (MET1: lexicographic ordering with decreasing weights, MET2: lexicographic ordering with increasing weights, MET3: the AHP method, MET4: the PROMETHEE method with the usual preference function, MET5: the PROMETHEE Method with the U-shaped preference function, MET6: the PROMETHEE method with the level preference function, MET7: the PROMETHEE method with the Gaussian preference function).*

For the meadow, tree, bare soil, and parking lot classes, the best individual classification accuracies are achieved by the PROMETHEE method using the Gaussian preference function and incorporating various criteria weights.

For the bitumen and brick roof classes, the best individual classification accuracies are achieved when applying the level preference function and various criteria weights to the PROMETHEE vector ordering method.

The proposed AHP-based vector ordering method yields the best individual classification accuracies for the water and asphalt land cover classes.

The individual test accuracies attained for the Pavia Center image by the different proposed vector ordering algorithms are presented in Figs. 5 and 6. Figure 5 shows the results obtained when using various criteria weights, while Fig. 6 shows the results obtained when using the same criteria weights.

From the results obtained in both experiments, the same conclusions can be drawn for both datasets.

– Combining spectral information with spatial information (i.e., morphological descriptors computed by the multivalued MP) improves the

Table 8: *Classification accuracies (percentage) attained by different vector ordering algorithms using various criteria weights for the Pavia Center image.*

Land Cover Classes	Reduced image (spectral classification)	Lexicographic ordering with decreasing bands weight	Lexicographic ordering with increasing bands weight	AHP with various criteria weights	PROMETHEE using the usual preference function with various criteria weights	PROMETHEE using the U-shaped preference function with various criteria weights	PROMETHEE using the level preference function with various criteria weights	PROMETHEE using the Gaussian preference function with various criteria weights
Asphalt	76.57	76.99	78.35	85.62	84.22	84.97	84.50	84.93
Meadows	36.06	41.39	38.57	46.39	42.19	43.09	45.81	48.21
Trees	75.41	79.60	77.09	80.02	79.40	79.84	79.75	82.17
Bare soil	82.32	90.21	89.70	90.76	82.58	84.43	87.16	92.08
Bitumen	75.03	82.08	77.47	83.97	82.67	82.48	84.00	83.43
Brick roofs	99.41	99.88	99.57	99.77	99.55	99.67	99.89	99.70
Parking lots	42.25	48.67	56.26	52.98	53.04	53.67	56.11	56.82
Water	96.03	96.97	96.16	98.01	96.26	96.90	97.29	97.30
OA	89.31	91.24	90.93	92.66	91.27	91.63	92.28	92.83
Kappa	0.85	0.88	0.87	0.90	0.88	0.88	0,89	0,90

Table 9: *Classification accuracies (percentages) achieved by different vector ordering algorithms using the same criteria weights for the Pavia Center image.*

Land Cover Classes	Reduced image (spectral classification)	Lexicographic ordering with decreasing bands weight	Lexicographic ordering with increasing bands weight	AHP with the same criteria weights	PROMETHEE using the usual preference function with the same criteria weights	PROMETHEE using the U-shaped preference function with the same criteria weights	PROMETHEE using the level preference function with the same criteria weights	PROMETHEE using the Gaussian preference function with the same criteria weights
Asphalt	76.57	76.99	78.35	79.09	77.13	77.64	78.16	80.03
Meadows	36.06	41.39	38.57	39.76	39.14	39.78	39.52	40.73
Trees	75.41	79.60	77.09	78.51	78.24	78.46	78.73	79.69
Bare soil	82.32	90.21	89.70	79.27	71.87	74.93	78.67	84.16
Bitumen	75.03	82.08	77.47	81.36	81.42	81.79	81.49	82.70
Brick roofs	99.41	99.88	99.57	99.61	99.47	99.57	99.68	99.63
Parking lots	42.25	48.67	56.26	50.34	45.20	46.51	50.93	49.91
Water	96.03	96.97	96.16	96.59	96.02	96.71	96.59	96.98
OA	89.31	91.24	90.93	90.69	89.52	90.13	90.65	91.28
Kappa	0.85	0.88	0.87	0.87	0.85	0.86	0.87	0.88

classification accuracy achieved for all the classes.

– Most of our proposed vector ordering methods attain improved classification accuracies over those of conventional methods, especially when incorporating the criteria weights into the multicriteria analysis architecture.

– The incorporation of various criteria weights results in greater classification improvements. This is because the inclusion of band weights renders the vector comparison system more realistic.

– Both PROMETHEE, which uses the Gaussian preference function, and the AHP produce more accurate results than do the other vector ordering algorithms.
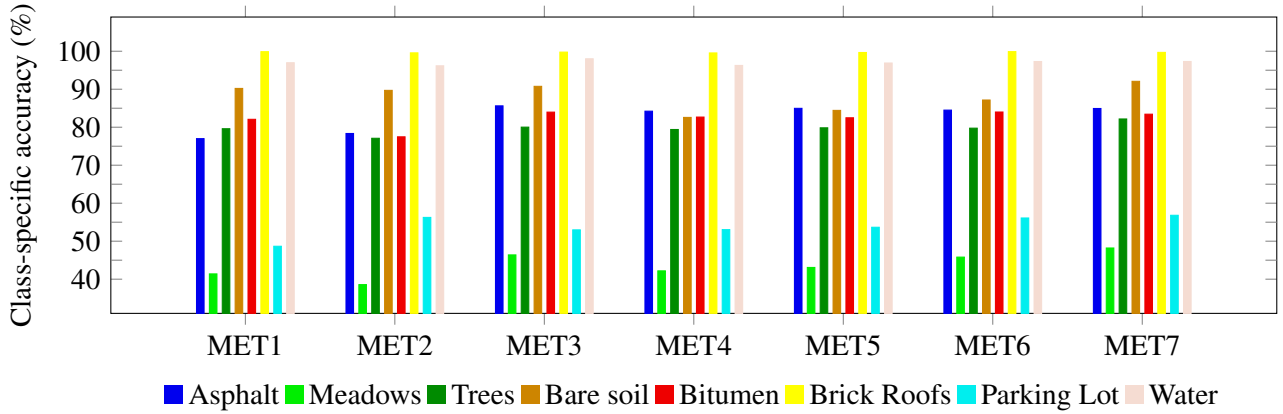
36

Fig. 5: *Individual test accuracies attained for the nine land cover classes in the Pavia Center scene dataset by different proposed vector ordering algorithms with various criteria weights (MET1: lexicographic ordering with decreasing weights, MET2: lexicographic ordering with increasing weights, MET3: the AHP algorithm using various criteria weights, MET4: the PROMETHEE algorithm using the usual preference function and various criteria weights, MET5: the PROMETHEE algorithm using the U-shaped preference function and various criteria weights, MET6: the PROMETHEE algorithm using the level preference function and various criteria weights, and MET7: the PROMETHEE algorithm using the Gaussian preference function and various criteria weights).*
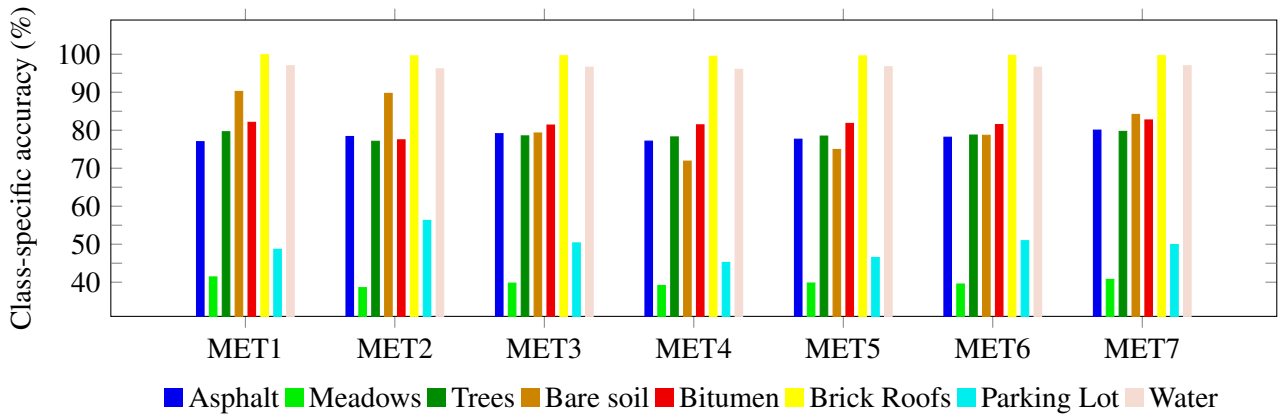

Fig. 6: *Individual test accuracies achieved for the nine land cover classes in the Pavia Center scene dataset by different proposed vector ordering algorithms with the same criteria weights (MET1: lexicographic ordering with decreasing weights, MET2: lexicographic ordering with increasing weights, MET3: the AHP algorithm using the same criteria weights, MET4: the PROMETHEE algorithm using the usual preference function and the same criteria weights, MET5: the PROMETHEE algorithm using the U-shaped preference function and the same criteria weights, MET6: the PROMETHEE algorithm using the level preference function and the same criteria weights, and MET7: the PROMETHEE algorithm using the Gaussian preference function and the same criteria weights).*

CONCLUSION

The multivalued mathematical morphology (MM) compares pixels in a predefined local neighbourhood using the supremum and infimum operators. However, there is no consensus on the total order relation for multivalued pixels, which is necessary for extending MM to multiband images. In this paper, we propose new vector ordering algorithms that use multicriteria analysis systems to obtain a vector ordering scheme

and extend MM to multiband images. The main idea of this work is to consider the vector ordering problem as a multicriteria analysis problem. To define our vector ordering scheme, we adapt two widely used and approved multicriteria analysis methods: the AHP and PROMETHEE. These methods compare actions that have multiple values to select the best action that satisfies the most criteria according to a predefined objective (maximization or minimization). In our context, they synthesize the vector components

into a unique numerical value that represents the vector priority and make vector comparisons possible. Thus, the proposed vector ordering algorithms are reduced vector ordering approaches. In the AHP method, we replace the Saaty preference scale with our preference scale, which expresses preferences in terms of distance, making it more suitable for our working context.

We apply the proposed vector ordering algorithms to two multiband images (Pavia University and Pavia Center images) to generate spatial descriptors using the multivalued MP. The spectral/spatial classification results exhibit improvements when using our proposed methods with various criteria weights compared to conventional vector ordering algorithms. This demonstrates the importance of considering the relative priority levels of the image bands during the ordering process. Furthermore, the proposed vector ordering algorithms preserve the initial vector set and guarantee the uniqueness of the vector extremes while also taking the correlations among the bands into account by processing multidimensional data simultaneously.

The PROMETHEE algorithm, which uses a Gaussian preference function, and the AHP algorithm provide more accurate classification rates than do all the other vector ordering algorithms. However, the proposed algorithms require the selection of a preference function that determines the vector outranking architecture.

The proposed vector ordering methods derived from a multicriteria analysis system are suitable for extending MM to multiband images.

In future research, we intend to include uncertainty and imprecision, which are two inherent parameters of satellite imagery analysis, in the AHP-based vector ordering algorithm. Additionally, we aim to explore other preference functions, such as V-shaped and linear functions, in the PROMETHEE vector ordering algorithm.

REFERENCES

Al-Otum HM (2003). Morphological operators for color image processing based on mahalanobis distance measure. Optical Engineering 42:2595–606.

Angulo J (2005). Unified morphological color processing framework in a lum/sat/hue representation. In: Mathematical Morphology: 40 Years On: Proceedings of the 7th International Symposium on Mathematical Morphology, April 18–20, 2005. Springer.

Angulo J (2007). Morphological colour operators in totally ordered lattices based on distances: Application to image filtering, enhancement and analysis. Computer vision and image understanding 107:56–73.

Angulo J (2010). Geometric algebra colour image representations and derived total orderings for morphological operators–part i: Colour quaternions. Journal of Visual Communication and Image Representation 21:33–48.

Aptoula E, Courty N, Lefèvre S (2014). An end-member based ordering relation for the morphological description of hyperspectral images. In: 2014 IEEE International Conference on Image Processing (ICIP). IEEE.

Aptoula E, Lefèvre S (2007). A comparative study on multivariate mathematical morphology. Pattern Recognition 40:2914–29.

Aptoula E, Lefevre S (2007). Pseudo multivariate morphological operators based on α-trimmed lexicographical extrema. In: 2007 5th International Symposium on Image and Signal Processing and Analysis. IEEE.

Aptoula E, Lefèvre S (2008a). α-trimmed lexicographical extrema for pseudo-morphological image analysis. Journal of Visual Communication and Image Representation 19:165–74.

Aptoula E, Lefèvre S (2008b). On lexicographical ordering in multivariate mathematical morphology. Pattern Recognition Letters 29:109–18.

Barnett V (1976). The ordering of multivariate data. Journal of the Royal Statistical Society Series A General 139:318–44.

Benediktsson JA, Palmason JA, Sveinsson JR (2005). Classification of hyperspectral data from urban areas based on extended morphological profiles. IEEE Transactions on Geoscience and Remote Sensing 43:480–91.

Benediktsson JA, Pesaresi M, Amason K (2003). Classification and feature extraction for remote sensing images from urban areas based on morphological transformations. IEEE transactions on geoscience and remote sensing 41:1940–9.

Brans JP, Vincke P, Mareschal B (1986). How to select and how to rank projects: The promethee method. European journal of operational research 24:228–38.

Brans JPV (1985). A preference ranking organization method: The promethee method for mcdm. Management Science 31:647–56.

Chanussot J, Lambert P (1998). Total ordering based on space filling curves for multivalued

morphology. Computational Imaging and Vision 12:51–8.

Chevallier E, Angulo J (2014). Image adapted total ordering for mathematical morphology on multivariate images. In: 2014 IEEE International Conference on Image Processing (ICIP). IEEE.

Chevallier E, Chevallier A, Angulo J (2016). N-ary mathematical morphology. Mathematical Morphology Theory and Applications 1.

Congalton RG (1991). A review of assessing the accuracy of classifications of remotely sensed data. Remote sensing of environment 37:35–46.

Congalton RG, Green K (2019). Assessing the accuracy of remotely sensed data: principles and practices. CRC press.

Dougherty ER (1992). An introduction to morphological image processing. In: SPIE. Optical Engineering Press.

Du Y, Chang CI, Ren H, D'Amico FM, Jensen JO (2003). New hyperspectral discrimination measure for spectral similarity. In: Algorithms and Technologies for Multispectral, Hyperspectral, and Ultraspectral Imagery IX, vol. 5093. SPIE.

Fauvel M, Benediktsson JA, Chanussot J, Sveinsson JR (2008). Spectral and spatial classification of hyperspectral data using svms and morphological profiles. IEEE Transactions on Geoscience and Remote Sensing 46:3804–14.

Franchi G, Angulo J (2015). Ordering on the probability simplex of endmembers for hyperspectral morphological image processing. In: Mathematical Morphology and Its Applications to Signal and Image Processing: 12th International Symposium, ISMM 2015, Reykjavik, Iceland, May 27-29, 2015. Proceedings 12. Springer.

Gao CJZXH, Hu XY (2013). An adaptive lexicographical ordering of color mathematical morphology. Journal of Computers 24:51–9.

Garcia A, Vachier C, Vallée JP (2008). Multivariate mathematical morphology and bayesian classifier application to colour and medical images. In: Image Processing: Algorithms and Systems VI, vol. 6812. SPIE.

Greco S, Figueira J, Ehrgott M (2016). Multiple criteria decision analysis, vol. 37. Springer.

Hanbury A, Serra JPF (2001). Mathematical morphology in the hls colour space. In: British Machine Vision Conference.

Keshava N (2004). Distance metrics and band selection in hyperspectral processing with applications to material identification and spectral libraries. IEEE Transactions on Geoscience and remote sensing 42:1552–65.

Lei T, Fan Y, Zhang C, Wang X (2013). Vector mathematical morphological operators based on fuzzy extremum estimation. In: 2013 IEEE International Conference on Image Processing. IEEE.

Lezoray O, Charrier C, Elmoataz A (2009). Rank transformation and manifold learning for multivariate mathematical morphology. In: 2009 17th European Signal Processing Conference. IEEE.

Lezoray O, Elmoataz A (2012). Nonlocal and multivariate mathematical morphology. In: 2012 19th IEEE International Conference on Image Processing. IEEE.

Li J, Li Y (2004). Multivariate mathematical morphology based on principal component analysis: initial results in building extraction. In: Proceedings of the 20th ISPRS, vol. 35. Citeseer.

Louverdis G, Vardavoulia MI, Andreadis I, Tsalides P (2002). A new approach to morphological color image processing. Pattern recognition 35:1733–41.

Nagel W (1988). Image analysis and mathematical morphology. volume 2: Theoretical advances. edited by jean serra. Journal of Microscopy 152:597–.

Plaza A, Martinez P, Pérez R, Plaza J (2002). Spatial/spectral endmember extraction by multidimensional morphological operations. IEEE transactions on geoscience and remote sensing 40:2025–41.

Plaza A, Martinez P, Perez R, Plaza J (2004). A new approach to mixed pixel classification of hyperspectral imagery based on extended morphological profiles. Pattern Recognition 37:1097–116.

Plaza A, Martínez P, Plaza J, Pérez R (2005). Dimensionality reduction and classification of hyperspectral image data using sequences of extended morphological transformations. IEEE Transactions on Geoscience and remote sensing 43:466–79.

Plaza J, Plaza AJ, Barra C (2009). Multi-channel morphological profiles for classification of hyperspectral images using support vector machines. Sensors 9:196–218.

Rosenfield GH, Fitzpatrick-Lins K (1986). A coefficient of agreement as a measure of thematic classification accuracy. Photogrammetric engineering and remote sensing 52:223–7.

Roy B, Bouyssou D, Jacquet-Lagrèze E, Perny P, Slowiński R, Vanderpooten D, Vincke P (2002). Aiding decisions with multiple criteria: Essays in

honor of Bernard Roy, vol. 44. Springer Science & Business Media.

Saaty RW (1987). The analytic hierarchy process—what it is and how it is used. Mathematical modelling 9:161–76.

Saaty T (2008). The analytic hierarchy process, mcgrawhill, new york, 1980. Akbari N and Zahedi Keyvan M Application of ranking approaches and MADAM decision making Tehran Country Municipalities Organization .

Sangalli M, Valle ME (2019). Approaches to multivalued mathematical morphology based on uncertain reduced orderings. In: Mathematical Morphology and Its Applications to Signal and Image Processing: 14th International Symposium, ISMM 2019, Saarbrücken, Germany, July 8-10, 2019, Proceedings 14. Springer.

Serra J (1986). Introduction to mathematical morphology. Computer vision graphics and image processing 35:283–305.

Serra J (1992). Anamorphoses and function lattices (multivalued morphology). in (dougherty, ed.) mathematical morphology in image processing. OPTICAL ENGINEERING NEW YORK MARCEL DEKKER INCORPORATED 34:483–.

Soille P (2013). Morphological image analysis: principles and applications. Springer Science Business Media .

Talbot H, Evans C, Jones R (1998). Complete ordering and multivariate mathematical morphology. Mathematical Morphology and its Applications to Image and Signal Processing :27–34.

Tarabalka Y, Benediktsson JA, Chanussot J (2009). Spectral–spatial classification of hyperspectral imagery based on partitional clustering techniques. IEEE transactions on geoscience and remote sensing 47:2973–87.

Tarabalka Y, Benediktsson JA, Chanussot J, Tilton JC (2010). Multiple spectral–spatial classification approach for hyperspectral data. IEEE Transactions on Geoscience and Remote Sensing 48:4122–32.

Van de Gronde J, Roerdink JB (2017). Nonscalar mathematical morphology. In: Advances in Imaging and Electron Physics, vol. 204. N/A: Elsevier, 111–45.

Van der Meer F (2006). The effectiveness of spectral similarity measures for the analysis of hyperspectral imagery. International journal of applied earth observation and geoinformation 8:3–17.

Vapnik V (1998). Statistical learning theory: New york etc.

Velasco-Forero S, Angulo J (2011). Supervised ordering in $\mathbb{R}_p$: Application to morphological processing of hyperspectral images. IEEE Transactions on Image Processing 20:3301–8.

Velasco-Forero S, Angulo J (2012). Random projection depth for multivariate mathematical morphology. IEEE Journal of Selected Topics in Signal Processing 6:753–63.

Velasco-Forero S, Angulo J (2014). Vector ordering and multispectral morphological image processing. Advances in low level color image processing :223–39.

Weber J, Lefevre S (2008). A multivariate hit-or-miss transform for conjoint spatial and spectral template matching. In: Image and Signal Processing: 3rd International Conference, ICISP 2008. Cherbourg-Octeville, France, July 1-3, 2008. Proceedings 3. Springer.